Assignment 8 - Renormalization groups.

Calandra Buonaura Lorenzo

(Dated: January 14, 2025)

In this study, we analize two computational techniques, the real-space renormalization group (RG) and the infinite density matrix renormalization group (iDMRG) and we apply them to the study of the transverse field Ising model. We compare the two methods approaches in terms of accuracy (comparison with exact diagonalization and mean field approximation), efficiency and computational time. The aim of the study is to show how these techniques can be used to simulate very big quantum systems, leveraging dimensionality reduction of the Hamiltonian.

1. INTRODUCTION

The Ising model is a fundamental theoretical framework, extensively used to study critical phenomena and phase transitions in lattice systems; it has been deeply studied from a theoretical point of view, and this makes it the perfect model to study using numerical techniques.

The first algorithm is the real-space renormalization group (RSRG) method, which provides a powerful tool for understanding critical behavior by systematically coarse-graining the system while preserving its essential physics. This approach has been revolutionary, allowing the numerical study of very large quantum systems (thermodynamical limit).

On the other hand, the density matrix renormalization group (DMRG) has emerged as a highly effective computational technique for one-dimensional quantum systems. In particular, the infinite DMRG (iDMRG) algorithm extends the RG framework, reaching higher precision in determining ground-state properties and low-energy excitations.

This study aims to compare and contrast the real-space RG and iDMRG approaches in the context of the Ising model: we analyze their respective strengths and limitations, focusing on their ability to capture critical behavior and their accuracy with respect to theoretical prediction.

2. THEORETICAL FRAMEWORK

This assignment studies how numerical algorithm can be implemented to simulate very big quantum system, leveraging renormalization groups. The model used as reference for the analysis is the transverse field Ising model, due to the possibility of comparison with exact solution of the system and the quantum phase transition that is present.

A. Transverse field Ising model

The transverse field Ising model (TFIM) is a 1D quantum spin system, defined on a lattice of N spins with a Hamiltonian given by:

$$\hat{H} = \sum_{i=1}^{N-1} \hat{\sigma}_i^x \hat{\sigma}_{i+1}^x - \lambda \sum_{i=1}^{N} \hat{\sigma}_i^z \tag{2.1}$$

where λ is the interaction strength between neighbour spins (considering only 1 neighbour interaction) and $\hat{\sigma}_i^z$ and $\hat{\sigma}_i^x$ are the Pauli spin operators for site i in the z- and x-directions, respectively [1]. As we can clearly see, the Hamiltonian is composed of two terms: the second term in Equation (2.1) represents the classical Ising interaction, favoring spin alignment in the z-direction (λ represents the strength of the external magnetic field). The first term, instead, introduces quantum fluctuations via the transverse magnetic field, which acts to flip the spins along the x-direction. The competition between these terms drives a quantum phase transition at a critical field strength, λ_c, where the system undergoes a transition from an ordered ferromagnetic phase to a disordered paramagnetic phase.

B. Quantum phase transition

As already announced, this model model exhibits a quantum phase transition as the transverse field λ is varied (we use the term 'quantum' to indicate that we are at zero temperature and the order parameter doesn't depend on T). To determine the critical point λ_c, we analyze the competition between the two terms in the Hamiltonian:

- In the classical limit where $\lambda = 0$, the Hamiltonian reduces to:

$$\hat{H}_{\text{classical}} = \sum_{i=1}^{N-1} \hat{\sigma}_i^x \hat{\sigma}_{i+1}^x. \tag{2.2}$$

  The ground state is characterized by long-range order in the x-direction, as the $\hat{\sigma}_i^x \hat{\sigma}_{i+1}^x$ term favors alignment of neighboring spins along the x-axis, which corresponds to a ferromagnetic phase.

- In the limit $\lambda \to \infty$, the Hamiltonian is dominated by the transverse field term:

$$\hat{H}_{\text{field}} = -\lambda \sum_{i=1}^{N} \hat{\sigma}_i^z. \tag{2.3}$$

The ground state in this limit is a product state where all spins align with the z-axis due to the strong transverse field, which corresponds to a paramagnetic phase.

The critical point λ_c is determined by the balance between the interaction term and the transverse field term: in particular, the exact critical point can be computed by mapping the Ising model to a 1D quantum chain of free fermions via the Jordan-Wigner transformation. After the transformation, the Hamiltonian becomes quadratic in fermionic operators, and the energy spectrum can be derived as:

$$E(k) = \pm\sqrt{(2\lambda - 2\cos k)^2 + (2\sin k)^2}, \tag{2.4}$$

where k is the momentum in the Brillouin zone. The energy gap ΔE closes at the critical point, which occurs when:

$$2\lambda - 2\cos k = 0 \quad \text{and} \quad 2\sin k = 0. \tag{2.5}$$

The gap closes at $k = 0$, giving:

$$2\lambda - 2 = 0 \quad \implies \quad \lambda = 1. \tag{2.6}$$

As we can see, we obtained that $\lambda_c = 1$; thus, we will expect that around that value the observable of the model will present some strange behaviour, which are sign of the phase transition [1].

C. Mean field approximation

The first analysis that can be performed for the quantum Ising model is the mean field approximation, which is based on the idea that the many-body wavefunction of the system can be approximated as a product of single-particle states, neglecting correlations between different sites, having:

$$|\psi_{\text{MF}}\rangle = \bigotimes_{i=1}^{N} |\psi_1\rangle = \bigotimes_{i=1}^{N} \sum_{\alpha_i=1}^{d} A_{\alpha_i} |\alpha_i\rangle, \tag{2.7}$$

where for a spin-1/2 system, $\alpha_i = \{\uparrow, \downarrow\}$ and $d = 2$.

Under this assumption, the system's energy can be computed as the expectation value of the Ising Hamiltonian in Equation (2.1); but since E_{MF} is extensive, it diverges in the thermodynamic limit ($N \to \infty$). However, the energy density $e = E/N$ is intensive, and in the thermodynamic limit, it can be calculated as:

$$e = -\left(\langle\psi_1| \hat{\sigma}_i^x |\psi_1\rangle\right)^2 + \lambda \langle\psi_1| \hat{\sigma}_i^z |\psi_1\rangle \equiv -r_x^2 + \lambda r_z, \tag{2.8}$$

where r_x and r_z are the two-level parameterizations in the Bloch sphere. To compute the ground state energy density of the Ising model within the mean field approximation, the above expression must be minimized with respect to r_x and r_z. The wavefunction normalization imposes the additional constraint:

$$r_x^2 + r_z^2 = 1. \tag{2.9}$$

Taking these considerations into account, it is possible to achieve the energy density as a function of the external field λ as:

$$e = \begin{cases} -1 - \frac{\lambda^2}{4}, & \lambda \in [-2, 2], \\ -|\lambda|, & \lambda \notin [-2, 2]. \end{cases} \tag{2.10}$$

This expression, though approximate, captures the system's physics by signaling two critical points, $\lambda = -2$ and $\lambda = 2$, where the second derivative of the energy density becomes discontinuous, suggesting a phase transition [2].

D. Real space RG

The first algorithm implemented is the real-space renormalization group (RSRG) method; this is an approximation technique based on the physical intuition that the ground state of a quantum system can be described using the low-energy states of its non-interacting bipartitions. This method allows the study of many-body quantum systems with large sizes N, up to the thermodynamic limit, leveraging dimensionality reduction of the Hamiltonian that describes the total system.

The algorithm proceeds as follows [2]:

0. **Initialization:** Consider a system with N sites that can be studied (diagonalized) numerically exactly and build the Hamiltonian $H_N : \mathbb{C}^{d^N} \to \mathbb{C}^{d^N}$.

1. **Diagonalization and projection:** Diagonalize H_N to find its eigenvalues and eigenvectors:

$$H_N = \sum_{i=1}^{d^N} E_i |E_i\rangle\langle E_i|, \tag{2.11}$$

where the eigenvalues E_i are in ascending order. Define the projector onto the lowest d_{eff} eigenstates as:

$$P = \sum_{i=1}^{d_{eff}} |E_i\rangle\langle E_i|. \tag{2.12}$$

Compute the projected Hamiltonian and operators in the reduced subspace:

$$\tilde{H}_N = P^\dagger H_N P, \quad \tilde{O} = P^\dagger O P. \tag{2.13}$$

2. **Construct enlarged system:** Build the Hamiltonian for a system of size $2N$ using the projected Hamiltonians $\tilde{H}_N$ for each bipartition and their interaction:

$$H_{2N} = \tilde{H}_N \otimes \mathbb{1} + \mathbb{1} \otimes \tilde{H}_N + \tilde{H}_{\text{int}}, \tag{2.14}$$

where the interaction term is given by:

$$\tilde{H}_{\text{int}} = \tilde{A}_N \otimes \tilde{B}_N, \tag{2.15}$$

with $\tilde{A_N} = P^\dagger A_N P$ and $\tilde{B_N} = P^\dagger B_N P$ and with $A_0 = \mathbb{1}_N \otimes \sigma_x$ and $B_0 = \sigma_x \otimes \mathbb{1}_N$.

3. **Iterate:** Repeat steps 1 and 2 until the desired system size is reached or convergence to the fixed point of the renormalization flow is achieved. At each step, the system size doubles ($N \to 2N$), while the dimension of the Hamiltonian representation is kept constant at d_{eff}.

We present also the pseudo-code of the algorithm in Algorithm 1, in order to achieve a better clarity. The implementation allows to save the energy density, as well as the dimension reached up to convergence; if convergence is not reached, the algorithm simply iterates `max_iter` times and then stops at the reached dimension.

Algorithm1 : Real Space RG (RSRG)

```
Require: $N, l, \tau, d_{eff}$, max_iter
Initialize: $H_N \leftarrow$ build Hamiltonian with (N, l) (2.1)
Initialize: $\epsilon_{prev} \leftarrow +\infty$
Initialize: $d_{curr} \leftarrow 2N$
Initialize: $A, B \leftarrow \mathbb{1}_{N-1} \otimes \sigma_z, \sigma_z \otimes \mathbb{1}_{N-1}$
while i $\leq$ max_iter do
    $H_{2N} \leftarrow$ compute $H_{2N}$ (2.14)
    $E, \psi \leftarrow$ diagonalize $H_{2N}$ (2.11)
    $P \leftarrow$ build projector (2.12)
    $E_0 \leftarrow E[0]$
    $\epsilon_{curr} \leftarrow E_0/d_{curr}$
    $\delta \leftarrow |\epsilon_{curr} - \epsilon_{prev}|$
    if $\delta > \tau$ then
        $H_N, A, B \leftarrow$ update operators (2.13)
    else
        break
    end if
    $\epsilon_{curr} \leftarrow 2\epsilon_{curr}$
    $\epsilon_{prev} \leftarrow \epsilon_{curr}$
end while
return $\epsilon_{curr}, E_0, \psi_0, d_{curr}$
```

E. Infinite DMRG

The second algorithm implemented is the infinite version of the density matrix renormalization group (DMRG), which is a powerful refinement of the original RG algorithm. In particular, it improves the truncation rule, achieving higher precision in the description of the system's final state, at the cost of slowing down the growth of the system size; unlike the original RG method, where the system size increases exponentially with the number of iterations (doubles at each iteration), the DMRG algorithm grows the system size linearly (we add two sites at each iteration).

The algorithm proceeds as follows [2]:

0. **Initialization and system grouping:** Consider the largest system size N that can be diagonalized exactly with reasonable computational resources. Group the N sites into two single sites in the middle and two groups of m sites on either side. The Hamiltonian of the system can be written as:

$$H_N = H_L^{(m+1)} + H_{\text{int}} + H_R^{(m+1)}, \tag{2.16}$$

where the Hamiltonians $H_L^{(m+1)} \equiv H_L^{(m+1)} \otimes \mathbb{1}_{m+1}$ and $H_R^{(m+1)} \equiv \mathbb{1}_{m+1} \otimes H_R^{(m+1)}$ refer to the left and right enlarged blocks, and $H_{\text{int}} \equiv \mathbb{1}_m \otimes H_{\text{int}} \otimes \mathbb{1}_m$ is the interaction Hamiltonian. The Hilbert space dimension of the system is $d^{2(m+1)}$, where d is the single-site dimension and m is the dimension of the grouped sites.

Diagonalizing H_N yields the ground state:

$$\left|E_0^N\right\rangle = \sum_{\beta_1,\beta_2} \psi_{\beta_1\beta_2} \left|\beta_1\right\rangle \left|\beta_2\right\rangle, \tag{2.17}$$

where $|\beta_i\rangle$ spans the basis of the left and right grouped sites.

1. **Density matrix construction:** Compute the density matrix of the ground state:

$$\rho_0^N = \left|E_0^N\right\rangle \left\langle E_0^N\right| \tag{2.18}$$

ant then the reduced density matrix for one half of the system (e.g., the left block):

$$\rho_L = \text{Tr}_R \rho_0^N \tag{2.19}$$

2. **Truncation** Diagonalize ρ_L:

$$\rho_L = \sum_{i=1}^{md} w_i \left|w_i\right\rangle \left\langle w_i\right|, \tag{2.20}$$

where w_i are the eigenvalues, ordered in descending order. Define the truncation projector:

$$P = \sum_{i=1}^{d_{eff}} \left|w_i\right\rangle \left\langle w_i\right|, \tag{2.21}$$

which reduces the Hilbert space from md states to d_{eff} states (we are keeping the largest d_{eff} eigenvectors, where d_eff is usually chosen equal to the starting size m).

3. **Effective Hamiltonian construction:** Use the projector P to compute the effective Hamiltonian for the system:

$$\tilde{H}_L^{(m+1)} = P^\dagger H_L^{(m+1)} P. \tag{2.22}$$

For the interaction term $H_{\text{int}} = \sum_k c_k A_k^L \otimes B_k^R$, project separately onto the left and right blocks:

$$\tilde{H}_{\text{int}} = \sum_k c_k \tilde{A}_k^L \otimes \tilde{B}_k^R, \tag{2.23}$$

where $\tilde{A}_k^L = P^\dagger A_k^L P$ and $\tilde{B}_k^R = P^\dagger B_k^R P$ and where $A_0^L = \mathbb{1}_m$ and $B_0^L = \mathbb{1}_{m-1} \otimes \sigma_x$.

4. **Iterate:** Repeat the steps above, replacing the left and right Hamiltonians with their effective forms. At each step, the system size increases by two sites, but the computational cost remains constant due to the fixed dimension m of the reduced Hilbert space.

As we can see, the key distinction between DMRG and traditional RG methods lies in the truncation rule: the infinite DMRG retains the states of the reduced density matrix with the highest populations, optimizing the overlap between the truncated and exact wavefunctions [2].

We present also the pseudo-code of the algorithm in Algorithm 2, in order to achieve a better clarity. The implementation allows to save the energy density, as well as the dimension reached up to convergence; if convergence is not reached, the algorithm simply iterates `max_iter` times and then stops at the reached dimension.

Algorithm2 : Infinite DMRG

```
Require: $m, l, \tau, d_{eff}$, max_iter
Initialize: $H_L, H_R \leftarrow$ Hamiltonian with (m, l) (2.1)
Initialize: $\epsilon_{prev} \leftarrow +\infty$
Initialize: $d_{curr} \leftarrow 2m + 2$
Initialize: $A_L, B_L, \leftarrow \mathbb{1}_m, \mathbb{1}_{m-1} \otimes \sigma_x$
Initialize: $A_R, B_R, \leftarrow \mathbb{1}_m, \sigma_x \otimes \mathbb{1}_{m-1}$
while i $\leq$ max_iter do
    $H_{L+1}, H_{R+1} \leftarrow$ compute partition Hamiltonians
    $H_{2m+2} \leftarrow$ compute $H_{2m+2}$ (2.16)
    $E_0, \psi_0 \leftarrow$ diagonalize $H_{2m+2}$ (2.17)
    $\rho_0 \leftarrow$ build density matrix (2.18)
    $\rho_L \leftarrow$ build reduced DM (2.19)
    $P \leftarrow$ build projector (2.21)
    $\epsilon_{curr} \leftarrow E_0/d_{curr}$
    $\delta \leftarrow |\epsilon_{curr} - \epsilon_{prev}|$
    if $\delta > \tau$ then
        $A_L, A_R, B_L, B_R \leftarrow$ update operators
        $A_L, A_R, B_L, B_R \leftarrow$ truncate operators (2.13)
    else
        break
    end if
    $\epsilon_{curr} \leftarrow 2 + \epsilon_{curr}$
    $\epsilon_{prev} \leftarrow \epsilon_{curr}$
end while
return $\epsilon_{curr}, E_0, \psi_0, d_{curr}$
```

3. CODE DEVELOPMENT

All the functions needed for the analysis have been collected into three python scripts, `ising_model.py`, `real_space_rg.py` and `infinite_dmrg.py`, which are then imported in a jupyter notebook for better visualization.

A. Ising model

Below is a concise summary of the functions implemented for the Ising model analysis:

- **pauli_matrices:** Builds and returns the Pauli matrices (σ_x, σ_y, σ_z) as sparse matrices.
- **ising_hamiltonian**: Constructs the Ising model Hamiltonian using sparse matrices.
- **diagonalize_ising)**: Diagonalizes the Ising Hamiltonian for various N and l values using sparse methods.

B. Real space RG

Below is a concise summary of the functions implemented for the real space RG analysis:

- **initialize_A_B:** Initializes the operators A_0 and B_0 using tensor products of the Pauli X matrix and identity matrices of size 2^N.
- **compute_H_2N:** Constructs the Hamiltonian H_{2N} for a system of size $2N$ by combining the input Hamiltonian H with interaction terms $A \otimes B$.
- **projector:** Computes the projection matrix based on the smallest d_eff eigenvalues and eigenvectors of the input Hamiltonian H.
- **update_operators:** Updates the effective Hamiltonian H_{eff} and operators A_{eff}, B_{eff} after projection using the projector matrix.
- **real_space_rg:** Iteratively applies real-space RG to compute the ground-state energy density and wavefunction for a system starting at size N, checking for convergence based on energy density differences.
- **update_hamiltonian:** Evaluates ground-state energy densities, eigenvalues, and wavefunctions for a range of coupling constants (λ), then stores results in dictionaries for further analysis.

C. Infinite DMRG

Below is a concise summary of the functions implemented for the infinite DMRG analysis:

- **initialize_operators:** Initializes operators A_L, B_L, A_R, B_R, and Hamiltonians H_L, H_R.
- **compute_H_LR:** Updates left and right block Hamiltonians H_{L1} and H_{R1}.
- **update_operators:** Updates A_L, B_L, A_R, B_R for a block with $m+1$ sites.
- **compute_H_2m:** Constructs full Hamiltonian H_{2m+2} for a $2m+2$ site system.
- **rdm:** Computes the reduced density matrix for a subsystem.
- **projector:** Constructs a projector using the d_{eff} largest eigenvectors of ρ_L.
- **truncate_operators:** Truncates operators and Hamiltonians using projectors P_L, P_R.
- **infinite_dmrg:** Iteratively applies infinite DMRG to compute the ground-state energy density and wavefunction for a system starting at size $2m+2$, checking for convergence based on energy density differences.
- **update_hamiltonian:** Evaluates ground-state energy densities, eigenvalues, and wavefunctions for a range of coupling constants (λ), then stores results in dictionaries for further analysis.

D. Code availability

All the data and the code for the data analysis can be found in this public Github repository: https://github.com/Kallo27/QIC/tree/main/Assignment8

4. RESULTS

The results are divided in three section; first we compare the implementation of both algorithms with the exact diagonalization, then we do the same for the mean field and finally we present a comparison between the two algorithms in terms of computational efficiency.

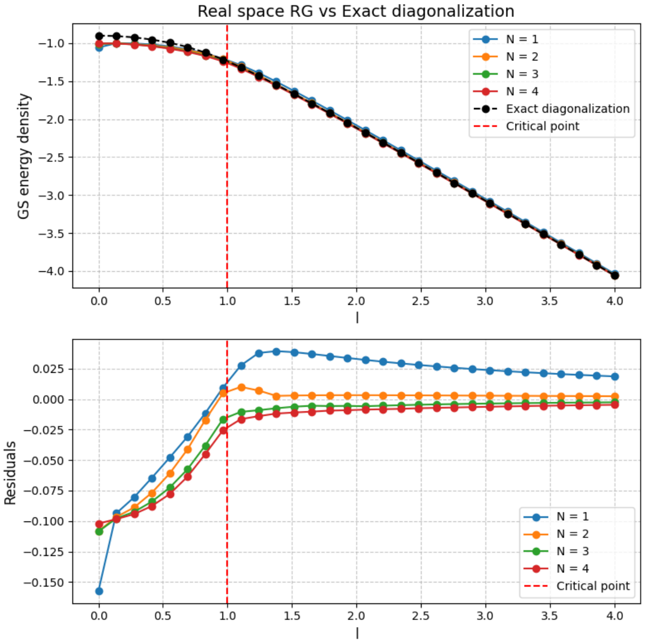

FIG. 1: RSRG vs exact diagonalization: (a) energy densities as function of λ, (b) residuals.

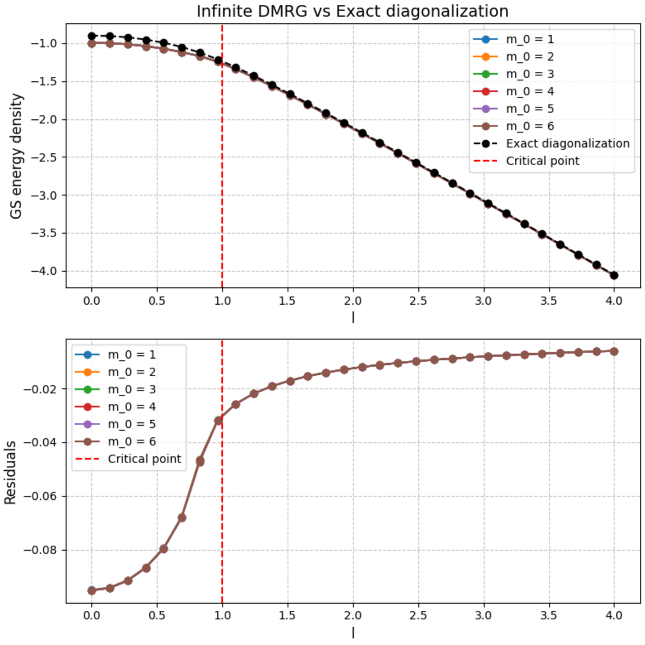

FIG. 2: DMRG vs exact diagonalization: (a) energy densities as function of λ, (b) residuals.

A. Exact diagonalization analysis

First of all, we consider a comparison between the exact diagonalization (for which we can arrive to a total system size of 15 spins) and the two implemented algorithms. This first analysis is crucial to understand whether the implementation is correct or not, as we want to be able to reproduce the exact behaviour of the system without loss. Figure 1 and Figure 2 depict the energy density and the residuals for different values of lambda and for different values of the initial quenched size, respectivley for the RSRG and the DMRG.

There are vary considerations that we can do looking at these graphs:

- First of all, we can see that the energy density in both cases is pretty much reproduced by the algorithm, meaning that the observed behaviour is in line with what expected.

- In both cases the residuals tend to 0 after the critical point: this can be explained simply from the fact that for big λ all the spins will tend to behave in the same way, so after the truncation the system will be very similar. On the other hand, when λ is small, the truncation introduces a bigger error, as the spins have all different behaviours.

- We can see that the absolute value of the residuals for the RSRG is bigger than for the DMRG: this is in line with what we expect, as the DMRG should be a more precise algorithm.

- From the residuals of the RSRG, we can clearly see that, as the quenched size increases, we reach a better approximation (as expected) and the system behaves more like the exact diagonalization.

- From the residuals of the DMRG, this same behaviour can not be observed, but this is because increasing the quenched size in this case simply adds two spins to the system, while in the RSRG it means doubling the whole chain.

From this considerations we can conclude that the implementation works fine, as it is pretty accurate and exhibits the quantum phase transition behaviour as wanted.

B. Mean field analysis

Then, we can proceed with the comparison with the mean field approximation; in this case, we don't want our model to behave like the mean-field, because we want it to be able to capture the interactions between neighbouring spins. Figure 3 and Figure 4 depict the energy density and the residuals for different values of lambda and for different values of the initial quenched size, respectivley for the RSRG and the DMRG.

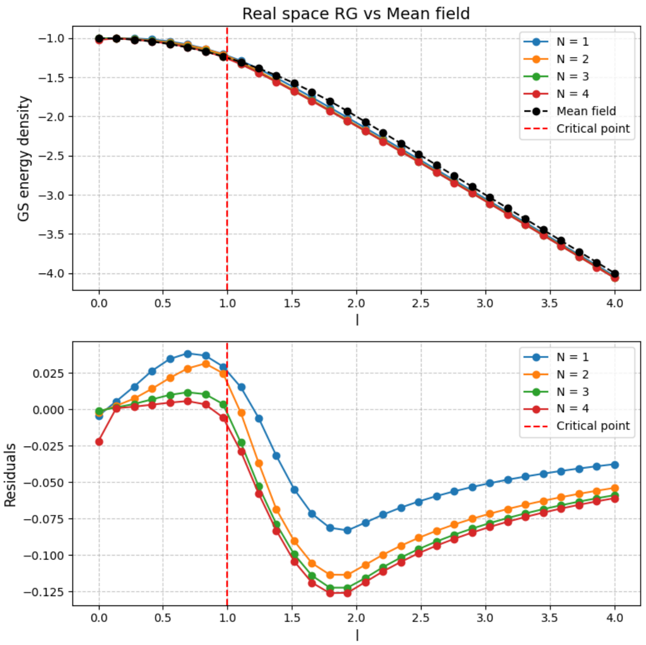

FIG. 3: RSRG vs mean field approximation: (a) energy densities as function of λ, (b) residuals.

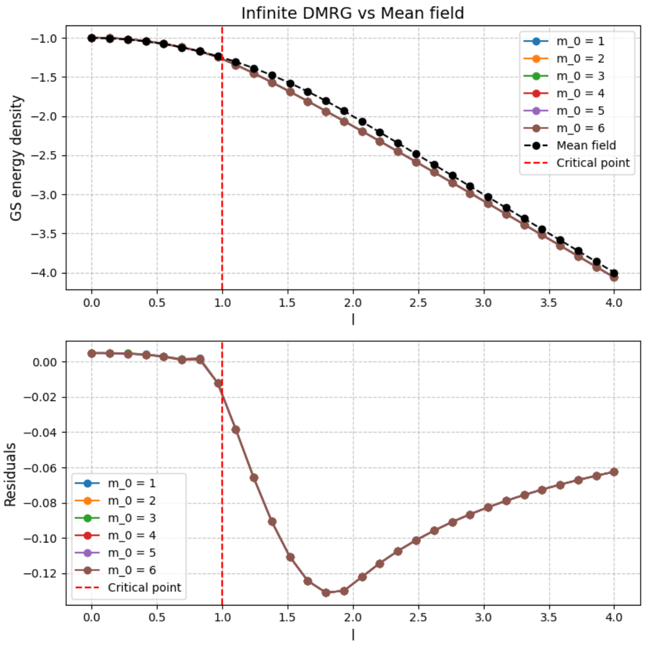

FIG. 4: DMRG vs mean field approximation: (a) energy densities as function of λ, (b) residuals.

Also in this case we can do some considerations about the presented graphs:

- First of all, both residuals present the phase transition at $\lambda = 1$, as expected. After this value the distance between the mean-field and both implementations increase.

- In opposition with what seen before, in this case we have that for small λ the algorithm reproduce better the mean-field approximation; this is in line with what previously underlined, i.e. the fact that the truncation procedure introduces a bigger error for a high entangled state.

- Similarly to what seen before, as we increase the quenched size in the RSRG we get further away from the mean field (and nearer exact diagonalization), while for the DMRG this behaviour is not observed due to the small variation in final size.

Thanks to these observations, we can conclude that the implementation of the two algorithms works correctly for values of $\lambda > 1$, while it introduces a more significant error for $\lambda \to 0$. Moreover, as expected, the infinite DMRG can reach a better precision than the real space RG, even if for smaller sizes of the total system.

C. Computational efficiency

Finally, we can compare the efficiency of the two algorithms. In order to do this, we set a convergence threshold for both algorithms and see which one converges before (see Figure 5). Also in this case we can clearly see the presence of a critical point for $\lambda \approx 1$, with two behaviours before and after this value. For both algorithms we see that the reached dimension for high λ is much smaller than for $\lambda \to 0$; this can still be explained by the fact that for high λ the truncation introduces a negligible error, which is instead more significative for small interaction strengths. Moreover, we can see that the reached dimension for small λ is much bigger for the RSRG rather than the DMRG; this is true, but it's not representative of the number of iterations, as the system doubles at every iteration for the RSRG, while increases linearly for the DMRG. If wee look to the number of iterations needed for convergence, for both regimes we have that the DMRG converges much slower than the RSRG, in agreement with the expectations.

This analysis could be continued studying the computational times of the two algorithms for different quenched sizes, but, due to lack of time, we could not do it. In any case the obtained results show that the DMRG is a more precise but slower algorithm than the RSRG.

5. CONCLUSION

In this study we implemented and analyzed two algorithms, the real space RG and the infinite version of the density matrix RG, to study the quantum phase transition in the transverse field Ising model.

From our analysis, we obtained that both RSRG and DMRG successfully reproduced the energy densities obtained from exact diagonalization, demonstrating the correctness of the implementations. The residuals confirmed that truncation errors are more pronounced for smaller λ, as the system is more entangled.

When compared to the mean field approximation, both algorithms displayed the expected deviation for $\lambda > 1$, confirming their ability to capture spin interactions. For $\lambda \to 0$, the truncation errors were more significant, but RSRG and DMRG still outperformed the mean field approximation in capturing the quantum phase transition.

In both cases, DMRG consistently showed better precision than RSRG, aligning with theoretical expectations, even if it required significantly more iterations to converge, particularly for small λ. RSRG, on the other hand, achieved faster convergence but at the cost of higher residuals.

Overall, the results confirm that both algorithms are effective tools for studying quantum phase transitions in the transverse field Ising model, each of them with its limit: while DMRG excels in precision, RSRG offers a computationally efficient alternative.

[1] A. P. Young, *The Transverse Field Ising Model*, Oxford University Press, 2009.

[2] S. Montangero, *Introduction to Tensor Network Methods*, Springer Nature Switzerland, 2018.

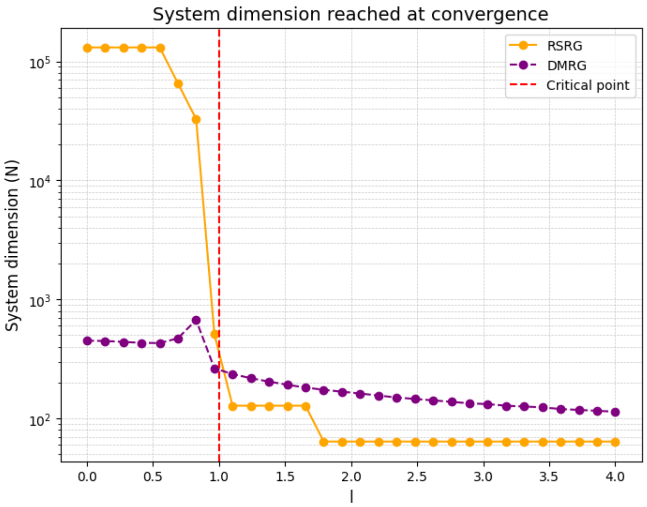

FIG. 5: System dimension reached for a fixed convergence threshold as a function of λ.